Available online at www.sciencedirect.com
ScienceDirect
Journal of Sound and Vibration 322 (2009) 851–869
JOURNAL OF SOUND AND VIBRATION
www.elsevier.com/locate/jsvi

Insights into the energy equipartition principle in large undamped structures

F. Magionesi[a], A. Carcaterra[b,c,*]

[a]INSEAN, Istituto Nazionale per Studi ed Esperienze di Architettura Navale, Via di Vallerano, 139, 00128 Rome, Italy
[b]Department of Mechanics and Aeronautics, University of Rome, 'La Sapienza', Via Eudossiana, 18, 00184 Rome, Italy
[c]Department of Mechanical Engineering, Carnegie Mellon University, Pittsburgh, PA 15213, USA

Received 14 January 2008; received in revised form 18 November 2008; accepted 25 November 2008
Handling Editor: C.L. Morfey
Available online 10 March 2009

Abstract

The question of energy sharing among complex engineering vibrating systems is still an open problem. On the basis of some recent investigations, this paper is addressed to the prediction of the equilibrium energies of interacting conservative resonators and to a better understanding of the principle of energy equipartition for large undamped systems. The analysis explores the field of linear and nonlinear vibrations, the effects of inhomogeneity, the weak or the strong coupling as well as the effect of the initial energy distribution among the subsystems. The principle of energy equipartition is shown to react in a different fashion to these factors. Some general arguments, supported by the results of numerical experiments, enlightening promoting or inhibiting factors to the reaching of energy equipartition conditions, are given.

1. The principle of energy equipartition in physics and engineering

This paper is conceived as part of a series of studies in the context of energy modeling of undamped complex structures [1–8] unloaded and subjected to initial conditions and, in particular, it is focused on the energy equipartition principle (EEP) as it is stated in statistical mechanics (SM) [9].

The ultimate goal is a better understanding of the limits of validity of the EEP in the context of engineering tools that make use of an energy-statistical approach to study undamped vibration problems. As far as the authors know, although several thermodynamic approaches have been developed in the last thirty years to attack structural engineering problems—e.g. statistical energy analysis (SEA) [10]—the problem of EEP has not received especial attention in the engineering literature.

The analysis of a system with a very large number of degrees of freedom generally implies the practical impossibility of a detailed description of its motion. This consideration led historically to produce a different way of tackling dynamic problems. In the context of molecular dynamics, a statistical approach—namely

*Corresponding author at: Department of Mechanics and Aeronautics, University of Rome, 'La Sapienza', Via Eudossiana, 18, 00184 Rome, Italy. Tel.: +39 06 50299268; fax: +39 06 5070619.
E-mail addresses: f.magionesi@insean.it (F. Magionesi), a.carcaterra@dma.ing.uniroma1.it (A. Carcaterra).

0022-460X/$ - see front matter © 2008 Elsevier Ltd. All rights reserved.
doi:10.1016/j.jsv.2008.11.038

statistical thermodynamics—is capable, in a relatively simple way, to provide expected values of relevant quantities, such as the energy [9,11]. The EEP plays in this frame a central role.

In fact, in its simplest form, the principle states that, in thermodynamic equilibrium conditions [9], a system of N particles with total energy E, exhibits a mean energy for each particle equal to $\bar{\varepsilon} = E/N$.

The question of the validity of the EEP has been, and still is, one of the subjects of interest in modern physics, starting from the famous FPU (Fermi–Pasta–Ulam) numerical experiment [12], in which the role of nonlinearities in the reaching energy equipartition and thermal diffusion conditions has been early investigated. More recently, several important studies have addressed the problem of inhomogeneous mass distribution in the atomic lattice [13] and the role of a threshold in the excitation of nonlinear effects [14] or finally the energy spreading among the lattice modes from higher to lower order modes as an effect of the nonlinearities [15].

Finally, the question related to Anderson localization (originally developed by Anderson in the context of diffusion in an atomic lattice and imported to engineering more recently by Hodges and Woodhouse [16]) seems to be relevant in this scenario. In particular it has been recently shown in Ref. [17], how the effect of mode localization can inhibit the acoustic energy diffusion with the inhibition of the mechanism leading to energy equipartition.

In the context of engineering, the analysis of very complicated systems, having a large number of degrees of freedom, reproduces conceptually the same difficulties met in molecular dynamics [1,2,10,18,19]. This is the case of many vibration problems for large aeronautic, aerospace or ship structures, where the size of the system is very large compared to the typical wavelengths induced by the exciting forces. In this frame, the practical importance of the EEP could rely in the simple prediction it provides of the energy distribution among the degrees of freedom of the considered system. In several cases, this information would be sufficient for characterizing the response of the system for many practical purposes.

Similar problems arise also for small scale engineering structures like micro/nano devices for which an analysis at molecular scale, implying the use of models with an extremely large number of degrees of freedom, is often coupled to more conventional macrostructural models [20,21].

The concept of equipartition is also used in the context of SEA as well as in the context of the theory of stochastic differential equations [22]. In both cases, although in different ways, EEP is associated with the modal energies for dissipative systems excited by random forces [23]. In this frame the EEP has a different nature and develops under completely different hypotheses than those considered in SM. This paper does not consider this last aspect of the EEP.

In SM the EEP is derived on the basis of the Gibbs–Boltzmann distribution using a number of assumptions not often satisfied for engineering systems. Some critical aspects related to a direct applicability of EEP as it is formulated in SM to engineering systems are shortly considered below.

- *Statistical characterization of the system*: The systems considered in SM are usually described in the phase space and are represented by a cloud of points moving over an equal-energy-surface. The statistical element of the theory appears with the introduction of the concept of ensemble. Tolman in Ref. [9] states: "we shall wish to consider the average behaviour of a collection of systems of the same structure as the one of actual interest but distributed over a range of different possible states". This is an ensemble of systems having the same Hamiltonian function. Each system of this ensemble consists of the same particles, the same interaction laws among the particles and has the same total energy as the others. The difference between them is only due to a different distribution of their representative points in the phase space, i.e. the systems of the ensemble have different initial conditions that spread over the same equal-energy-surface.
  However, in engineering problems uncertainty in initial conditions is only one of the possible aspects of uncertainty. Moreover, in general, structural engineers are mostly concerned with an ensemble of systems that do not have the same structure, but rather present uncertainties in their constructive parameters affecting the inherent response of each sample of the collection. In this case, the Hamiltonians associated to each system are different: this is not the kind of uncertainty claimed in SM.
- *Equiprobability hypothesis and the microcanonical ensemble*: In SM, under stationary conditions, the hypothesis of a uniform probability of finding representative points of the ensemble of systems over the equal-energy-surface in the phase space is assumed. Such an ensemble is called microcanonical [9,11].

This element represents the statistical characterization of the ensemble, i.e. it is the *a priori* probabilistic information characterizing the investigated random process. This leads to investigate a very narrow class of systems and too specific to cover the practical interests of engineering vibration. Thus, a suitable modification of this assumption must be introduced developing a statistical energy method for engineering structures as illustrated in Refs. [1,2].

- *Energy decomposability*: SM predicts the energy partitioning between two coupled subsystems in steady-state conditions through the Gibbs–Boltzmann distribution. The two considered subsystems are supposed to be weakly coupled. This means that the total energy of the whole system is just the sum of the partial energies of the subsystems, i.e. the energy associated to the interaction forces is negligible with respect to the energy stored in each subsystem. Some authors in the field of SM call this hypothesis principle of energy decomposability [11]. This is often a critical aspect in engineering problems, where the case of strong coupling between interacting systems is indeed frequently met and the coupling energy is not in general negligible.

2. Energy equipartition for linear homogeneous systems

The concept of energy equipartition is here initially considered in the light of the results presented in Refs. [1,2]. In that analysis—named time asymptotic ensemble energy average (TAE)—the unsteady energy sharing between two coupled linear resonators, each consisting of a very large number of degrees of freedom (or modes) is considered in the context of modal analysis from an engineering point of view. Moreover, a statistical approach is also introduced considering an ensemble of systems, following in this sense the SM inspiration. The theory allows to determine the time history of the ensemble average energies of the subcomponents together with the general relationship between power flow and the expected energies of the two subsystems.

As a particular result, the analysis also provides the long term energy responses of the two subcomponents, at least in the case of undamped linear systems. This result is shown to be coincident with the EEP only under particular circumstances, but it does not seem to be a general rule.

For the sake of clearness, some basic elements of the theory developed in Ref. [1] are briefly illustrated.

S is a force-free, conservative, N degrees of freedom system, satisfying given initial conditions, and its motion is described by the vector $\mathbf{w}$. Two subparts of S, S_1 and S_2, are considered such that $S \equiv S_1 \cup S_2$.

Let be $\mathbf{\Phi}_i$ and $q_i(t)$ the orthonormal modes and the Lagrangean coordinates of S, respectively, and t the time. Vibration of S_1 and S_2 is described by

$$\mathbf{w}^{(1)}(t) = \sum_{i=1}^{N} \mathbf{\Phi}_i^{(1)} q_i(t); \quad \mathbf{w}^{(2)}(t) = \sum_{i=1}^{N} \mathbf{\Phi}_i^{(2)} q_i(t) \tag{1}$$

where the displacement vector has been decomposed as

$$\mathbf{w} = \begin{Bmatrix} \mathbf{w}^{(1)} \\ \mathbf{w}^{(2)} \end{Bmatrix}$$

and the two sub-vectors $\mathbf{w}^{(1)}$ and $\mathbf{w}^{(2)}$ refer to the displacement of the masses belonging to S_1 and S_2, respectively. Correspondingly, the mass and the stiffness matrices ($\mathbf{M}$ and $\mathbf{K}$) and the *i-th* eigenvector are partitioned as follows:

$$\mathbf{M} = \begin{bmatrix} \mathbf{M}_{11} & \mathbf{M}_{12} \\ \mathbf{M}_{21} & \mathbf{M}_{22} \end{bmatrix} \quad \mathbf{K} = \begin{bmatrix} \mathbf{K}_{11} & \mathbf{K}_{12} \\ \mathbf{K}_{21} & \mathbf{K}_{22} \end{bmatrix} \quad \mathbf{\Phi}_i = \begin{Bmatrix} \mathbf{\Phi}_i^{(1)} \\ \mathbf{\Phi}_i^{(2)} \end{Bmatrix} \tag{2}$$

The total energy E of the system S reads

$$E = \frac{1}{2}\dot{\mathbf{w}}^{\mathrm{T}}\mathbf{M}\dot{\mathbf{w}} + \frac{1}{2}\mathbf{w}^{\mathrm{T}}\mathbf{K}\mathbf{w} = \frac{1}{2}\sum_{r,s=1}^{2} \dot{\mathbf{w}}^{(r)^{\mathrm{T}}}\mathbf{M}_{rs}\dot{\mathbf{w}}^{(s)} + \mathbf{w}^{(r)^{\mathrm{T}}}\mathbf{K}_{rs}\mathbf{w}^{(s)} \tag{3}$$

In this expression the energy in the summation can be grouped in three different contributions: those for which $r=s=1$, those for which $r=s=2$ and the remaining ones $r\neq s$. We define the energy associated with S_1 the part associated with $r=s=1$, i.e. the part of the energy depending only on the degrees of freedom related to S_1.

Let $\alpha_{ij}^{(r)}=\boldsymbol{\Phi}_i^{(r)\mathrm{T}}\mathbf{M}_{rr}\boldsymbol{\Phi}_j^{(r)}$, $\beta_{ij}^{(r)}=\boldsymbol{\Phi}_i^{(r)\mathrm{T}}\mathbf{K}_{rr}\boldsymbol{\Phi}_j^{(r)}$, then the energies of S_1 and S_2 are $E^{(1)}(t)$, $E^{(2)}(t)$, respectively, obtained as the sum of both the kinetic and potential contributions:

$$E^{(r)}(t)=\frac{1}{2}\sum_{i,j=1}^{N}\alpha_{ij}^{(r)}\dot{q}_i(t)\dot{q}_j(t)+\frac{1}{2}\sum_{i,j=1}^{N}\beta_{ij}^{(r)}q_i(t)q_j(t) \tag{4}$$

where expressions (4) hold if the mixed energy terms $\frac{1}{2}\boldsymbol{\Phi}_i^{(r)T}\mathbf{M}_{rs}\boldsymbol{\Phi}_j^{(s)}$, $\frac{1}{2}\boldsymbol{\Phi}_i^{(r)T}\mathbf{K}_{rs}\boldsymbol{\Phi}_j^{(s)}$ with $r\neq s$ are negligible. This implies that the physical coupling between the two subsystems stores a negligibly small amount of energy. Under this assumption, the sum of the energies $E^{(1)}(t)+E^{(2)}(t)$, each of them determined by using Eq. (4), provides the total energy stored into the whole system S.

The orthonormality conditions imply the equalities

$$\alpha_{ij}^{(1)}+\alpha_{ij}^{(2)}=\delta_{ij}\quad \beta_{ij}^{(1)}+\beta_{ij}^{(2)}=\omega_i^2\delta_{ij} \tag{5}$$

Assume that the system S satisfies the initial conditions $\mathbf{w}(\mathbf{x},0)=0$, $\dot{\mathbf{w}}(\mathbf{x},0)=\dot{\mathbf{w}}_0(\mathbf{x})$. The Lagrangean coordinates are

$$q_i(t)=A_i\,\sin\,\omega_i t,\quad A_i=\frac{1}{\omega_i}\int_S\rho\dot{\mathbf{w}}_0\cdot\boldsymbol{\Phi}_j\,\mathrm{d}V \tag{6}$$

The explicit time dependency of the energy with respect to time is obtained as

$$E^{(r)}(t)=\sum_{i,j=1}^{N}[a_{ij}^{(r)}\,\cos(\omega_i+\omega_j)t+b_{ij}^{(r)}\,\cos(\omega_i-\omega_j)t] \tag{7}$$

where

$$a_{ij}^{(r)}=\tfrac{1}{4}A_iA_j(\alpha_{ij}^{(r)}\omega_i\omega_j-\beta_{ij}^{(r)})\quad b_{ij}^{(r)}=\tfrac{1}{4}A_iA_j(\alpha_{ij}^{(r)}\omega_i\omega_j+\beta_{ij}^{(r)}) \tag{8}$$

Suppose that inherent uncertainties affect the system S. As a consequence, expression (7) is not deterministic anymore, representing indeed a stochastic process. The attention is addressed to the population of energies $E^{(1)}(t)$, $E^{(2)}(t)$ and more precisely to the time history of the ensemble average of this population.

The uncertain system S is described through its natural frequencies ω_i, regarded as a set of random variables, characterized by a joint probability density function (pdf) $p(\omega_1,\omega_1,\ldots,\omega_N)=p(\Omega)$. Thus, the ensemble energy average of the subsystem S_1 is

$$\bar{E}^{(1)}(t)=\int_0^\infty\int_0^\infty\cdots\int_0^\infty E^{(1)}p(\omega_1,\omega_2,\ldots,\omega_N)\,\mathrm{d}\omega_1\,\mathrm{d}\omega_2\ldots\mathrm{d}\omega_N=\int_{R^N}E^{(1)}p(\Omega)\,\mathrm{d}\Omega \tag{9}$$

where $\mathrm{d}\Omega=\mathrm{d}\omega_1\,\mathrm{d}\omega_2\ldots\mathrm{d}\omega_n$; an analogous expression is valid for the second subsystem S_2.

Substitution of Eq. (7) into Eq. (9) and considering only the steady-state energy component (the time independent contribution), i.e. the equilibrium energies $\bar{E}_{eq}^{(1)}$, $\bar{E}_{eq}^{(2)}$, of the system S_1 and S_2, yields [1]:

$$\begin{aligned}\bar{E}_{eq}^{(1)}&=\lim_{t\to\infty}\bar{E}^{(1)}(t)=\sum_{i=1}^{N}\int_R\Pi_i(\omega_i)b_{ii}^{(1)}(\omega_i)\,\mathrm{d}\omega_i\\ \bar{E}_{eq}^{(2)}&=\lim_{t\to\infty}\bar{E}^{(2)}(t)=\sum_{i=1}^{N}\int_R\Pi_i(\omega_i)b_{ii}^{(2)}(\omega_i)\,\mathrm{d}\omega_i\end{aligned} \tag{10}$$

with $\Pi_i(\omega_i)=\int_{R^{N-1}}p(\Omega)\,\mathrm{d}\Omega_i$, $\mathrm{d}\Omega_i=\mathrm{d}\Omega/\mathrm{d}\omega_i$.

Eqs. (10) provide the expected energy approached asymptotically, i.e. at late times in the sense explained in Ref. [1].

It is interesting to explore the chance of simplifying these expressions. In Ref. [1] it is proven, under the hypothesis of one homogeneous system (e.g. a homogeneous cavity, plate, rod or beam) partitioned in two

subsystems, that the following expressions can be obtained:

$$\bar{E}_{eq}^{(1)} = \frac{N^{(1)}}{N}\bar{E}_0, \quad \bar{E}_{eq}^{(2)} = \frac{N^{(2)}}{N}\bar{E}_0 \tag{11}$$

where $N^{(1)}$ and $N^{(2)}$ ($N^{(1)}+N^{(2)}=N$) are the number of modes of S_1 and S_2, respectively, contained into the frequency range $[0,\omega_{\max}]$, where $\omega_{\max}$ is the frequency associated to the highest order mode included into the system model.

This expression states that, under steady conditions, the energy per mode of each subsystem is equal to the initial energy per mode of the whole system. This expresses a condition reminiscent of the EEP. However, this principle does not seem to hold in general but only under the particular conditions specified above.

3. The validity of the energy equipartition for general engineering systems

The analysis presented in this section shows how the EEP is, in general, a property that is rarely satisfied in dynamical systems. The hypotheses that allow its deduction in the frame of Statistical Thermodynamics are hardly realized in engineering systems. Moreover, in most of cases it is even difficult to check if the requirements needed to use the EEP are met or not in the analysed case. Therefore, in the present section, the conditions that can lead to the appearance of EEP are examined and classified, as far as possible, as inhibiting or promoting factors for the reaching of energy equipartition conditions.

These factors arise from a combined examination of the literature in engineering as well as in physics. The previous section has shown that the EEP holds under the hypotheses that the two resonators are (i) linear, (ii) homogeneous, (iii) weakly coupled and subjected to a (iv) point power injection. In the analysis ahead, the role of each of these hypotheses on the appearance of the EEP is considered investigating systematically the effects of the factors listed below:

- Inhomogeneity of the subsystems.
- Initial energy distribution among the subsystems.
- Nonlinearities in the constitutive relationships.
- Degree of coupling between subsystems.

They seem, in different form, potential responsible for promoting or inhibiting the EEP in dynamical systems and their effect is examined separately in the next subsections for systems of engineering interest.

The cases analysed in the following sections consider N-degrees of freedom systems, connected through linear or nonlinear springs. The masses are located along a line (1D case), or over a plane (2D case), or occupy a volume (3D case). The form of the equations of motion of these systems can be also interpreted as the discrete representation of continuous systems, basically described by 1D, 2D or 3D wave equations (with possible nonlinearity), associated, for example, to rods, acoustic pipes, acoustic volumes etc.

A final question concerns the analysis of the single case versus the analysis of some ensemble average to check the validity of EEP. In this respect, it must be noticed that the use of ensemble averages, as in statistical thermodynamics as well as, e.g. in Ref. [1], is only a useful tool aimed at simplifying the theoretical analysis. Thus, when producing direct numerical simulations, is more interesting to look directly at the single case, the one of actual interest for the designer. However, as shown in Ref. [1], for systems equipped with a large number of degrees of freedoms, as those here considered, deviations of the single case from the ensemble average are expected to be small. For these reasons, in the following the single case analysis is considered, avoiding any ensemble average.

As a preliminary step, some quantitative parameters to estimate the deviation of the energy distribution from the one predicted by the EEP are introduced, based on an internal statistics of the single case and not on ensemble average considerations.

3.1. Estimators for the deviation from the EEP

The energy pdf is the basis for checking deviations from the EEP, as well as the related energy statistical moments, especially those of first and second order. The energy e, associated with each individual degree of

freedom of the investigated system S, allows the definition of an energy pdf $p(e)$ such that

$$n(e_1, e_2) = N \int_{e_1}^{e_2} p(e)\,\mathrm{d}e \tag{12}$$

where $n(e_1,e_2)$ represents the number of degrees of freedom of the system having expected energy within the interval $[e_1,e_2]$.

Thus,

$$\int_0^E p(e)\,\mathrm{d}e = 1 \tag{13}$$

where E is the energy of the whole system.

The examination of this function permits of estimating deviations with respect to the EEP. In this context, the first and the second-order energy moments, $\bar{e}$ and σ_e^2, respectively, have special importance:

$$\bar{e} = \int_0^E ep(e)\,\mathrm{d}e, \quad \sigma_e^2 = \int_0^E (e-\bar{e})^2 p(e)\,\mathrm{d}e \tag{14}$$

It is natural to compare $\bar{e}$ with the value $\bar{\varepsilon}$ that provides the value predicted by the EEP, while σ_e^2 expresses the deviation with respect to $\bar{e}$. Both provide indication on the correctness of the EEP. In those cases for which $\bar{e} \equiv \bar{\varepsilon}$, that however is not necessarily the rule as it will be clarified ahead, σ_e^2 provides a measure of the dispersion of the energy data around the average value $\bar{\varepsilon}$ predicted by the EEP.

Frequently the partitioning of the investigated system S into a number M of subsystems is useful, each collecting a certain number N_k of degrees of freedom of S. Thus, besides σ_e^2 that relates to the energy of each degree of freedom, a global deviation estimator σ_E^2 can be considered providing information about the deviation of the energy $E^{(k)}$ of each subsystem with respect to the value $N_k\bar{\varepsilon}$ expected by the EEP. In this case:

$$\sigma_E^2 = \sum_{k=1}^{M} \frac{(E^{(k)} - N_k\bar{\varepsilon})^2}{M} \tag{15}$$

Note that in the numerical simulations, the energies e as well as $E^{(k)}$ are time dependent and consequently $p(e)$ and the related statistical estimators $\bar{e}$, σ_e^2 and σ_E^2 are also time dependent.

3.2. Test cases

Three different systems are considered to perform numerical simulations testing the validity of Eq. (11).

The first test case is performed on a rod, with a total length $L = 1$ m, subdivided into two subsystems of length $1/4L$ and $3/4L$, respectively, as shown in Fig. 1a.

The simulation is performed using a finite difference scheme with 2000 points. The discretized investigated system corresponds to the coupling of two chains of masses, connected with springs. The first system consists of 500 masses and the second of 1500 masses.

The second tested system is a square membrane (as shown in Fig. 1b), with area 1 m^2, ideally subdivided by a clamp line into two systems with area 0.275 and 0.725 m^2, respectively.

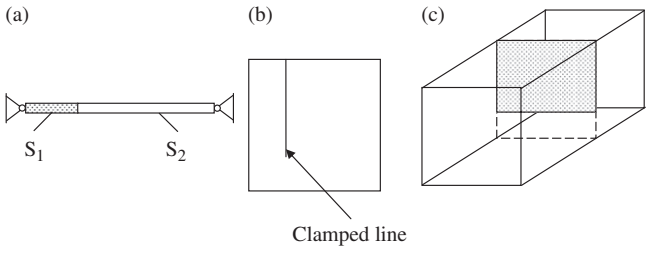

Fig. 1. Setup: (a) the 1D, (b) the 2D and (c) the 3D setup.

The related numerical equations are solved using a finite difference scheme with a total number of 1600 degrees of freedom. The discretized system corresponds to a lattice structure divided into two subsystems with 440 and 1160 masses connected through springs.

Finally, the last test case is a 3D cubic acoustic cavity with a volume $1\,m^3$, subdivided into two cavities by a rigid rectangular panel, as shown in Fig. 1c. The side of the panel is shorter than the sides of the box, leaving a rectangular opening between the two subsystems. The volumes of the two cavities are in the ratio 1:2.5.

A finite difference scheme with grid $24 \times 24 \times 24$, corresponding to 13 824 degrees of freedom, is used for the numerical solution of the acoustic wave equation. The discretized system corresponds to the coupling of two 3D lattices, with 3950 and 9874 masses, respectively.

3.3. Inhomogeneity effects

Different sets of numerical simulations were performed for the aforementioned test cases (1D, 2D, and 3D systems) to explore the effects of inhomogeneity on the reaching of the energy equipartition condition.

The first test case is performed on a 1D system (Fig. 1a). The rod is subdivided into two homogeneous subsystems with Young modulus $E = 1\,N\,m^2$ and mass per unit length $\rho = 1\,kg\,m^{-1}$. The initial conditions are given by

$$\begin{aligned} u(x,0) &= 0, \\ \dot{u}(x,0) &= \delta(x - x_0) \end{aligned} \tag{16}$$

where u and $\dot{u}$ are the rod's displacement and velocity, δ the Dirac delta function and x_0 is the point of application of the velocity spike, given as initial condition.

The discretized system corresponds to couple two linear chains of 500 and 1500 masses, respectively, each of them equal to $5 \times 10^{-3}\,kg$, connected with linear springs, all with the same stiffness equal to $1\,N\,m^{-1}$.

In Fig. 2, the time histories of the two homogeneous subsystem energies are shown and compared with the theoretical results, obtained by applying Eq. (11). The agreement between these results is asymptotically good.

For comparison, an inhomogeneity effect is introduced. The masses per unit length of the first and second systems are now different and equal to 2×10^{-3} and $1 \times 10^{-4}\,kg$, respectively. The obtained results are displayed in Fig. 2. In this case the ratio between the subsystem energies is equal to 1.5:1. The result does not agree with the prediction given by Eq. (11), i.e. with the EEP prediction, which provides indeed the ratio 3:1.

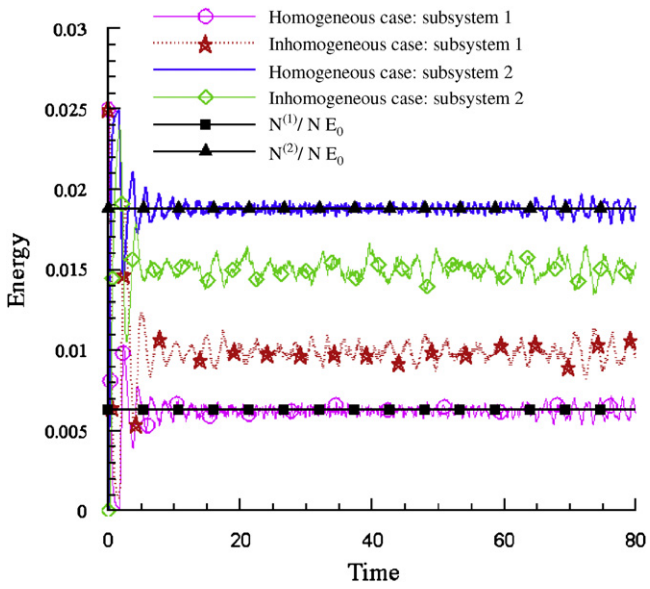

Fig. 2. 1D-homogeneous and inhomogeneous test cases.

In Figs. 3 and 4 the comparison of the deviation parameters σ_E^2 and σ_e^2, defined in Section 3.1, for the previous homogenous and inhomogeneous cases are depicted.

In the homogeneous case, the global deviation σ_E^2 exhibits an initial decrease at early times, where an energy sharing among the substructures takes place. An asymptotic very low value is indeed reached in the equilibrium condition, which matches with the prediction of the EEP (i.e. Eq. (11)). On the contrary, in the inhomogeneous case, besides the fact that $\bar{\varepsilon} \neq \bar{e}$, the spreading around the actual mean energy value $\bar{e}$ is large even asymptotically.

The second sets of numerical simulations are performed on a square membrane with a side of length $L = 1\,\mathrm{m}$, a density $\rho = 1\,\mathrm{kg\,m^{-2}}$, and divided into two systems with different area, see Fig. 1b. Initial conditions are given as in the previous case by a velocity spike at some point. The discretized system is a 2D lattice partitioned into two homogeneous subsystems having 440 and 1160 masses, respectively, each of them with a mass value equal to $6.25 \times 10^{-4}\,\mathrm{kg}$, and connected through springs with the same stiffness, equal to $1\,\mathrm{N\,m^{-1}}$. In Fig. 5 the time histories of the subsystem energies are shown and compared with the asymptotic energy values predicted applying the EEP. The numerical results are in good agreement with the theoretical results provided by Eq (11).

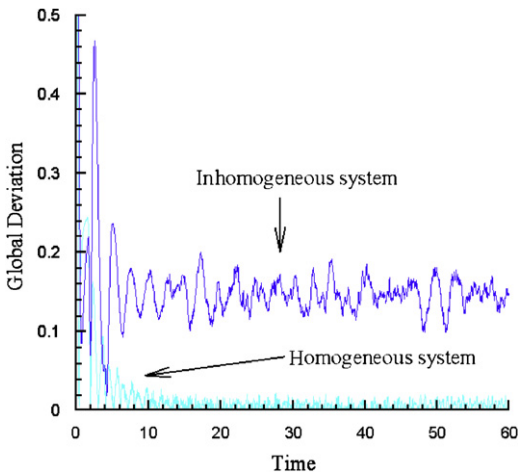

Fig. 3. 1D-global deviation parameter for the homogeneous and inhomogeneous systems.

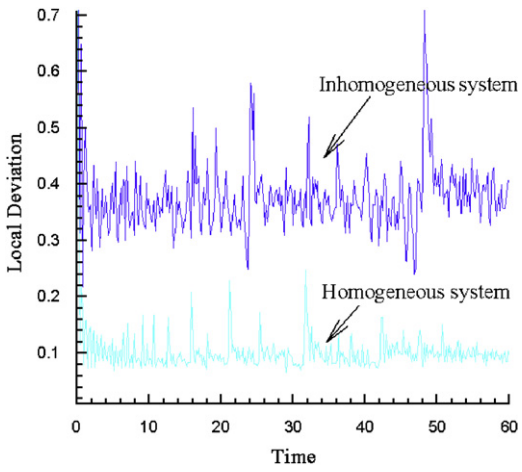

Fig. 4. 1D-local deviation parameter for the homogeneous and inhomogeneous systems.

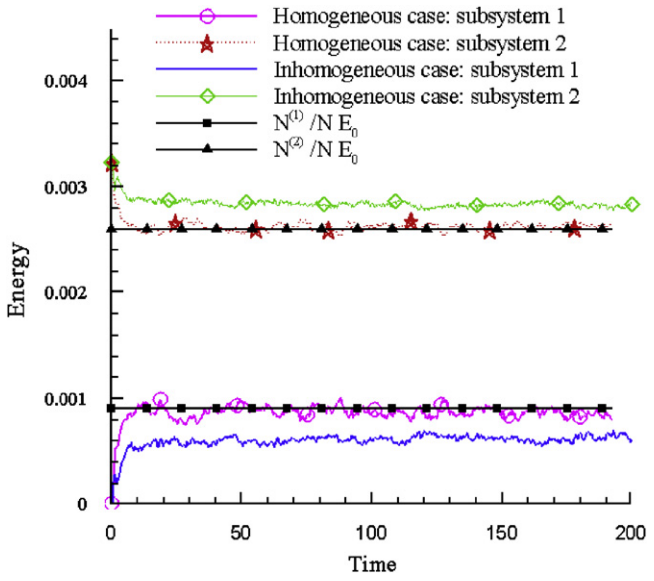

Fig. 5. 2D-homogeneous and inhomogeneous test cases.

As already done for the 1D test case, an inhomogeneity effect is introduced through a variation of the subsystem densities. The first system, characterized by a density equal to $2\,\mathrm{kg\,m^{-2}}$, has 440 masses each equal in the present case to $1.25\times10^{-3}\,\mathrm{kg}$, while the second system has the same characteristics as in the previous test. In Fig. 5 the energy time histories of the inhomogeneous subsystems are shown and compared with the asymptotic energy values predicted by Eq. (11). It appears that, as for the 1D system, the inhomogeneity effect produces a discrepancy between the numerical results and the EEP prediction. The time histories of the global and local deviation parameter are in this case not displayed, being t heir trend for the homogeneous and inhomogeneous case totally similar to the results shown in Figs. 3 and 4.

Finally, the last test case is performed on the 3D cubic acoustic cavity. The initial condition consists of a velocity spike at some point inside the first subsystem (chamber 1 in Fig. 1c). The discretized system corresponds to the coupling of two 3D lattices, divided into two subsystems with 3950 and 9874 masses, respectively, with a mass value equal to $7.23\times10^{-5}\,\mathrm{kg}$. The obtained energy time histories of the homogeneous subsystems, shown in Fig. 6, match satisfactorily with the EEP prediction represented by Eq (11).

Introducing an inhomogeneity, such that each mass is set equal to $1.44\times10^{-4}\,\mathrm{kg}$ for the first chamber and $7.23\times10^{-4}\,\mathrm{kg}$ for the second chamber, it appears from Fig. 6 that the energy time histories do not match the values obtained by applying the EEP (Eq. (11)).

From the obtained results it is concluded that the presence of an inhomogeneity in the system tends to inhibit the reaching of energy equipartition conditions.

3.4. Initial energy distribution

The same three test cases analysed in the previous section are here used to understand the influence of the initial energy distribution among the two subsystems in the reaching of a condition of energy equipartition.

In the previous section the velocity spike initial condition produces a broad band distribution of the initial energy among the system's modes. In this section the initial energy is indeed trapped in a narrower band. For the homogeneous rod (see Fig. 1a), the initial displacement of the first subsystem is selected to match its

second uncoupled mode:

$$u(x,0) = \begin{cases} \sin\left(\dfrac{2\pi x}{L_1}\right) & x < L_1 \\ 0 & x > L_1 \end{cases}$$
$$\dot{u}(x,0) = 0 \tag{17}$$

where L_1 is the length of the first subsystem.

The simulations are performed using the same finite difference scheme described in the previous section, that permits a direct comparison of the energy time histories for the two sets of initial conditions. In Fig. 7 the energies of the two subsystems are shown and compared with the theoretical results obtained by applying Eq. (11). The results of Fig. 7 compared with those of Fig. 2 show how the initial energy distribution largely affects the energy time history. The energy trend matches quite well the EEP predictions only if the initial energy is rather uniformly spread among the system's mode (velocity spike condition), while when only a local

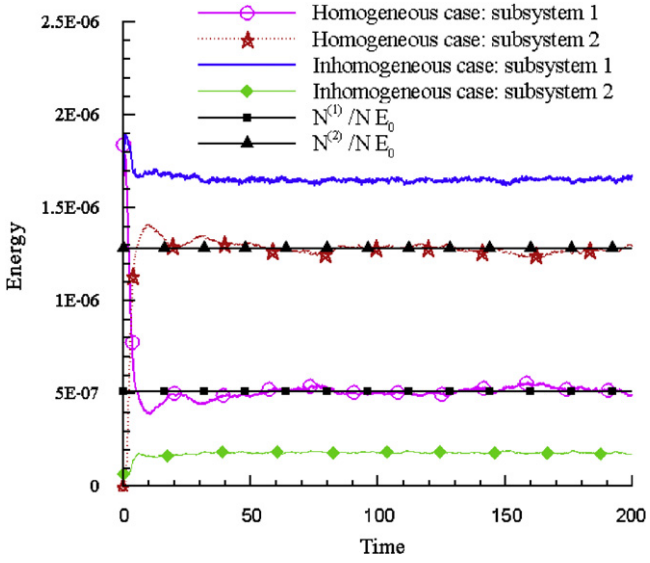

Fig. 6. 3D-homogeneous and inhomogeneous test cases.

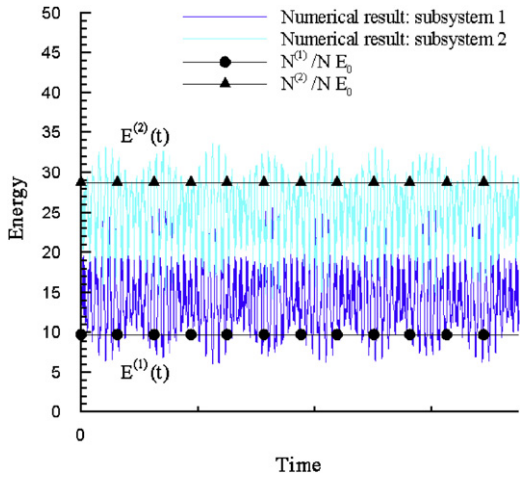

Fig. 7. 1D-local mode initial deformation.

mode is excited by the initial conditions, a larger deviation from the mean energy is observed and even the mean energy value does not match anymore the EEP theoretical prediction.

An analogous type of initial condition (initial displacement of the first subsystem matching its second uncoupled mode) is used for the 2D and 3D test cases (see Figs. 8 and 9). The results confirm the dependency of the energy distribution between the two subsystems on the initial conditions.

In Fig. 10 a comparison of the global deviation parameter for the three test cases under analysis is shown. Notwithstanding a clear decrease of this parameter is observed passing from the 1D test case to the 3D one, the deviation from the EEP is much smaller when the initial condition consists of a velocity spike rather than exciting only a local mode.

As a final point, the energy distribution among each degree of freedom for a 1D homogeneous system is analysed. In Figs. 11 and 12 the energy value of each mass (i) of the system is evaluated as a function of the time for two different initial conditions corresponding to a spike velocity and a local mode excitation, respectively.

If the EEP would be valid, the value of the mean energy should be equal for each degree of freedom and equal to $\bar{\varepsilon}$. For the velocity spike initial condition (see Fig. 11), after a short transient ($t>6$ s), the energy is convected along the rod with a tendency to produce a uniform distribution.

On the contrary, as shown in Fig. 12, if the initial condition matches a local mode of the structure, the EEP does not hold, with an energy distribution substantially periodic. The results show, in general, that the energy

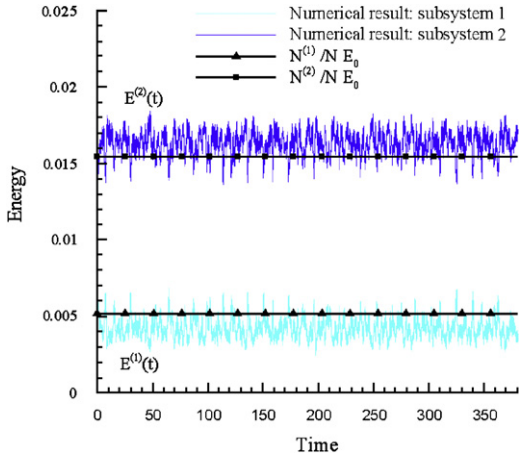

Fig. 8. 2D-local mode initial deformation.

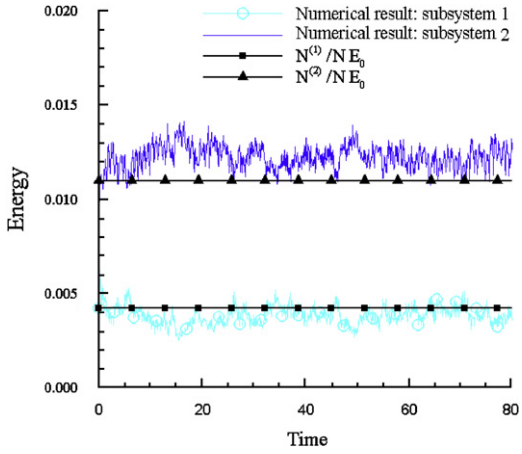

Fig. 9. 3D-local mode initial deformation.

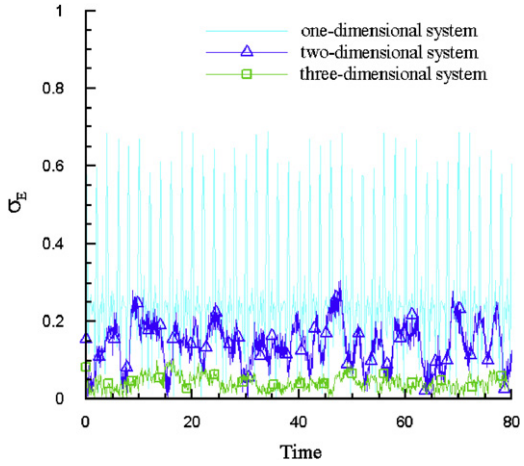

Fig. 10. Global deviation parameter for a local mode initial deformation.

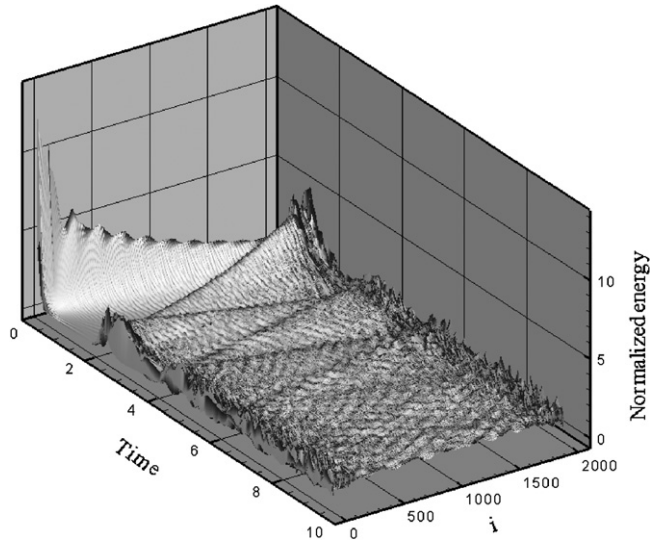

Fig. 11. 1D-energy distribution among the degrees of freedom for a velocity spike initial condition.

equipartition is largely affected by the initial energy distribution. When the initial conditions excite the modes in a broad frequency band, then the EEP holds, but it substantially fails if only few modes are excited by the initial conditions.

3.5. Nonlinearity

It is reasonable to expect that a nonlinearity in the elastic constitutive relationship produces a coupling effect among the system modes making the related energy sharing process more effective, thus approaching the EEP in a closer way.

The first set of numerical simulations is performed on the 1D system described in the previous sections. A cubic nonlinearity is introduced in the elastic constitutive relationship as $\sigma = E\varepsilon + \gamma\varepsilon^3$, where σ and ε are stress and deformation, respectively and γ is a suitable material coefficient initially set equal to $3 \times 10^{-3}\,\mathrm{N\,m^2}$.

The first test considers the homogeneous system subjected to a velocity spike. The results of this analysis are not reported in this paper, being identical to those the linear case.

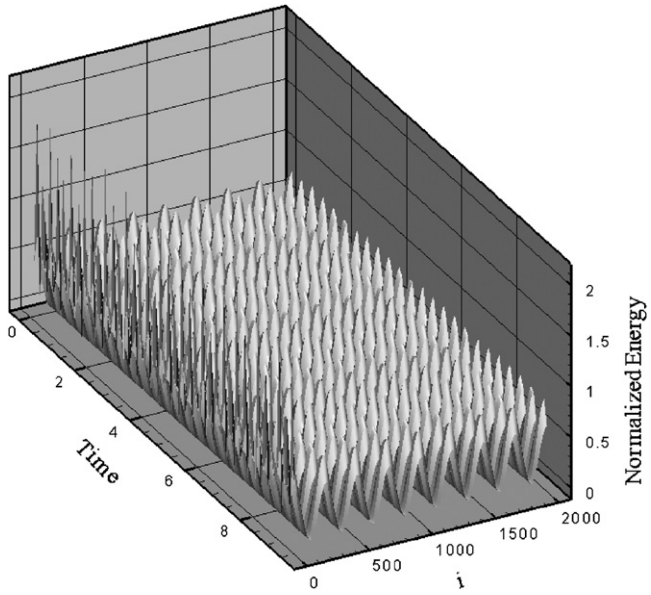

Fig. 12. 1D-energy distribution among the degrees of freedom for a local mode initial deformation.

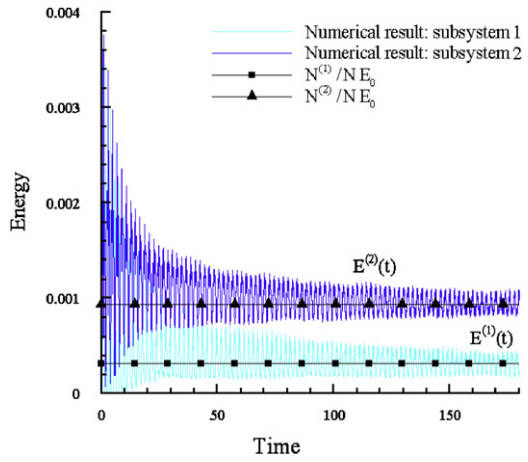

Fig. 13. 1D-nonlinear system, local mode initial deformation.

The second test considers indeed a local mode initial deformation (as the one shown in the previous section). In this case the energies, depicted in Fig. 13, after a transient, reach their asymptotic values, which coincide with the results obtained by applying the EEP, contrarily with respect to the linear case (see Fig. 7). Furthermore, the energy fluctuations around the mean are more rapidly reduced with respect to the linear case, as shown in Fig. 13.

In Figs. 14 and 15, a comparison of σ_E and σ_e for the linear and nonlinear rods is shown. The two cases show totally different behaviours. In fact, while for the linear system the global deviation is higher and presents large fluctuations, for the nonlinear system both the amplitude and the fluctuations decrease rapidly with the time.

Moreover, the inhomogeneous case is considered, and the results match again satisfactorily those predicted by the EEP, i.e. Eq. (11), in contrast with the linear case, as shown in Fig. 16. The conclusion is that inhomogeneity plays against equipartition more effectively in linear systems than in the nonlinear ones.

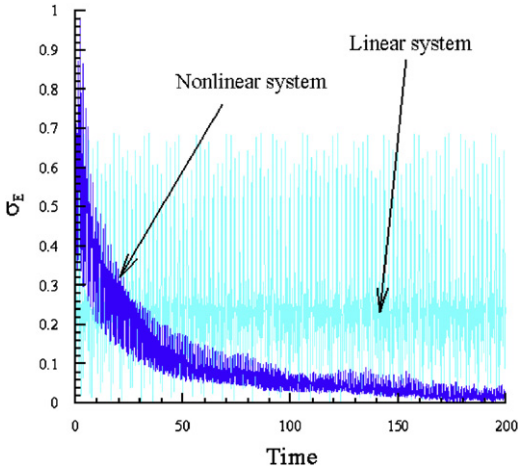

Fig. 14. 1D-comparison of the global deviation parameter for linear and nonlinear systems.

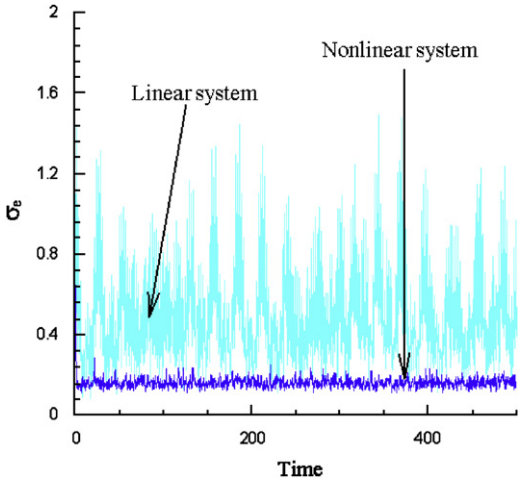

Fig. 15. 1D-comparison of the local deviation parameter for linear and nonlinear systems.

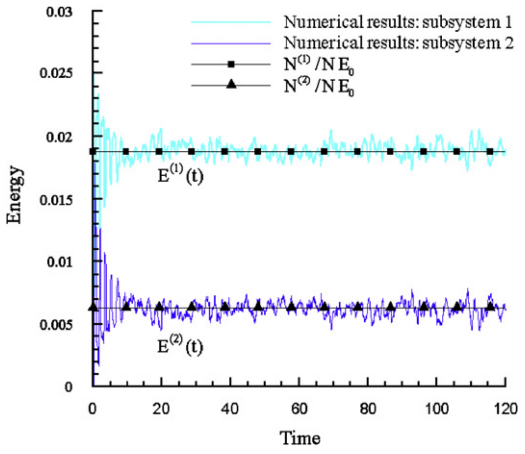

Fig. 16. 1D-nonlinear inhomogeneous system.

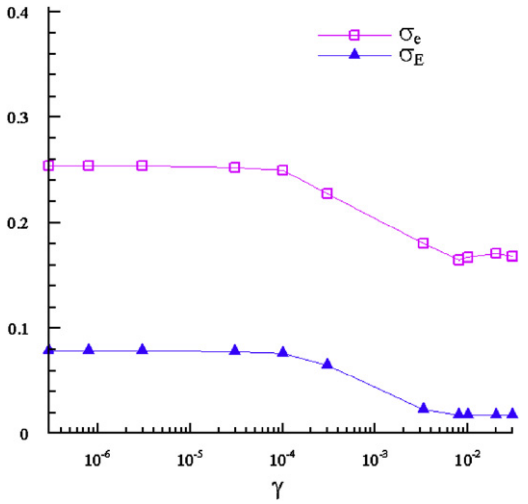

Fig. 17. 1D-local and global deviation parameters as function of γ.

Finally, a set of numerical simulations are performed on the 1D test case, varying the value of γ, i.e. the strength of the nonlinearity. The global and local deviation parameters, σ_E and σ_e, are evaluated for different values of γ and the results are displayed in Fig. 17.

It appears that both σ_E and σ_e show a sudden decrease when the strength of the nonlinearity is higher than a threshold value. This means that the EEP is approached only for γ large enough, i.e. only when the involved nonlinearity is sufficiently high to produce a significant modal energy coupling. Note that all the previous simulations are preformed with a value of γ larger than the threshold level.

The same tests, although they are not reported in this paper, are performed on the 2D and 3D systems, leading to analogous conclusions.

It is interesting to remark that the nonlinear system tends more effectively to energy equipartitioning. The physical reason relies in the modal coupling due to the nonlinear interaction. In fact, linear systems have decoupled modes, meaning that the energy initially stored in a given mode remains confined within it. This modal energy localization property is not indeed preserved in nonlinear systems. The energy initially conferred to some particular mode is spread over a larger number of modes, because of their coupling. As a consequence, a spatial spreading of the energy over the whole structure is also produced. Consider for example a single mode initial excitation. The modal shape is characterized by a non-uniform amplitude spatial distribution, clearly apparent by the presence of nodes and peaks. Thus, in this case, that is typical for linear systems for single mode excitation, an energy equipartition among the degrees of freedom is not observed. However, in the presence of the nonlinearity, the modal coupling spreads the energy over several modes, and their contributions along the structure overlap; nodes as well as peaks do not appear anymore, thus producing an equalization effect in the system energy response.

3.6. Degree of coupling among subsystems

In SM a fundamental assumption is that the coupling among the subsystems is "weak", i.e. in Khinchin's terminology the system must verify the "*decomposability principle*" [11]. This assumption basically expresses that the energy of a system is just the sum of the energy of the substructures that compose the system itself; consequently, the energy associated to the interaction forces is negligible with respect to the energy stored in each subsystem. This leads to a paradox [11] for which, strictly following the theory and the "*decomposability principle*", any energetic interaction between the subsystems would be excluded and the energy would remain wholly within the subsystem initially excited. Thus, in SM the weak coupling condition is a necessary approximation to develop the whole theory, EEP included.

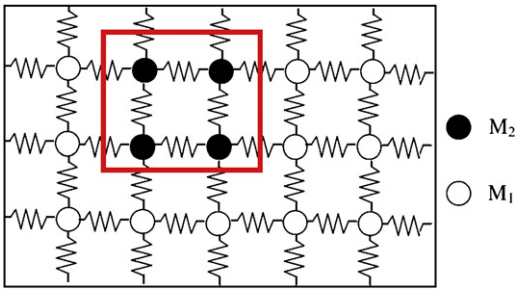

Fig. 18. 2D lattice.

For this reason in this paper a set of numerical simulations is performed to better understand the influence of the coupling strength on the energy partitioning among the subsystems. The investigated model corresponds to a 2D lattice composed by M masses. This lattice is partitioned in two homogeneous subsystems: a square sub-lattice S_2, consisting of M_2 masses, is cut out from whole system. The remaining M_1 masses of the lattice produce the sub-lattice S_1 ($M = M_1 + M_2$). The two subsystems defined in this way are coupled through linear springs, as depicted in Fig. 18.

The degree of energy coupling η between S_1 and S_2 is defined as the ratio between the energy stored within the coupling springs and the characteristic energy level of the subsystems, namely assumed equal to the lowest energy value between S_1 and S_2:

$$\eta = \frac{E_{coupling}}{\min\{E_1, E_2\}} \tag{18}$$

The degree of coupling η can be varied considering different partitions of the lattice, i.e. modifying the number of the masses included into S_2.

If the EEP would be valid, the potential energy e_i stored in each spring would be the same. In this case it is easy to demonstrate that the potential energy stored in the N_c junction springs is equal to

$$E_{coupling} = \sum_{i=1}^{N_C} e_i = 4N \cdot e_i \tag{19}$$

where N is the number of masses belonging to the side of the square sub-lattice S_2, while the potential energy stored by the N_1 springs inside S_2 is given by

$$E_2 = \sum_{i=1}^{N_1} e_i = 2(N-1)Ne_i \tag{20}$$

Finally, the potential energy of the sub-lattice S_1 is

$$E_1 = 2(N_{TOT} - 1)N_{TOT}e_i - 2(N-1)Ne_i \tag{21}$$

being N_{TOT} the number of masses along the side of the sub-lattice S_1. Consequently, under the hypothesis of energy equipartition, the degree of coupling assumes one of the two following expressions:

$$\eta = \frac{E_{coupling}}{E_2} = \frac{2}{(N-1)} \quad \text{or} \quad \eta = \frac{E_{coupling}}{E_1} = \frac{2N}{(N_{TOT}-1)N_{TOT} - (N-1)N} \tag{22}$$

depending on the smallest value between E_1, E_2.

This means that, when the EEP is valid, η is only a function of the dimension of the subsystems.

A single simulation is performed assuming a velocity spike in S_1 as initial condition. A set of results is then obtained for different values of η achieved through the variation of M_1 and M_2, being their sum always equal to M, which implies a variation of the energy stored in each subsystem and in the coupling springs.

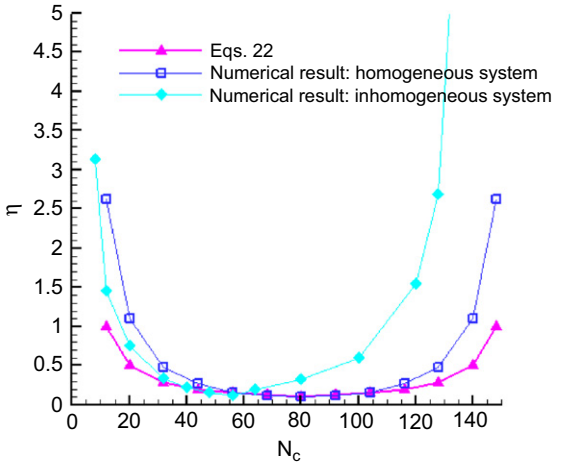

Fig. 19. Degree of coupling for homogeneous and inhomogeneous systems.

Table 1
Summary of the obtained results.

	Weak	Strong
Inhomogeneity	+	−
Degree of coupling	+	−
Non linearity	−	+
Initial energy distribution: spreading on the modes	−	+

The results of this analysis are shown in Fig. 19 and are compared with the one deduced from the EEP and given by Eqs. (22). In the abscissa there is the number of coupling springs N_c between the two subsystems, while on the y-axis is η. It is evident that, for low values of η, the EEP (given by Eqs. (22) and represented by the curve with triangles) and the numerical results (based indeed on the actual values of the energies and represented by the curve with squares) are in good agreement, but as soon as the coupling becomes stronger, the numerical curve departs from that provided by Eqs. (22).

A similar numerical experiment is performed for an inhomogeneous system, where the masses of S_1 and S_2 are now different (compare the curve with triangles and that with diamonds depicted in Fig. 19).

In Fig. 19, the degree of coupling for different number of connecting springs obtained numerically are compared with the theoretical results given by the EEP. The results does not differ from those obtained in the homogeneous system, except to a lost of symmetry of the numerical trend.

This analysis confirms the key role assumed by the strength of the coupling upon the achievement of the EEP.

4. Conclusions

The present paper discusses the validity of the EEP. On the basis of the numerical experiments illustrated in the previous sections some general qualitative conclusions can be drawn.

Table 1 summarizes very schematically the obtained results. The different elements reported in the first column, are classified as promoting (+) or inhibiting (−) factors for the reaching of an energy equipartition condition relating them to their weak or strong presence in the considered system.

The general conclusion can be synthesized as follows: homogeneous systems, weakly coupled, with localized (spike) initial excitation behave more closely to the prediction of the EEP. However, this is true if the system is linear; the presence of a nonlinearity large enough acts indeed as a very effective equalizer of the energy among

the degrees of freedom of the system, such that strongly nonlinear systems match reasonably well the EEP prediction even in the presence of inhomogeneity and strong coupling or initial conditions that store the energy in correspondence of a few number of modes.

A last remark concerns the differences observed among 1D, 2D or 3D systems. It has been observed in the large number of performed simulations that, in general, higher dimensional systems match closely the energy equipartition. The dimensionality of the system has an implication on the degree of connectivity of the masses among them. For the kind of systems here investigated, the 1D structure provides for each mass of the chain just an interaction with two other neighboring masses, while each mass of the 2D structure interacts with four masses and for the 3D system each mass interacts with six other masses. It can be concluded that also the degree of connectivity of the system tends to act as a promoting factor for energy equipartition.

The present analysis suggests that the EEP is far to represent a general model for energy distribution in mechanical systems. However, for engineering structures having special characteristics it can be an effective and simple predictive tool for their energy response.

Acknowledgement

This work has been support by the Ministero dei Trasporti in the frame of ''Programma Ricerche INSEAN 2007–2009''.

References

[1] A. Carcaterra, Ensemble energy average and energy flow relationships for nonstationary vibrating systems, *Journal of Sound and Vibration* 288 (2005) 751–790 (special issue ''Uncertainty in Structural Dynamics'').
[2] A. Carcaterra, Time asymptotic ensemble energy-average: modelling the energy dynamics of uncertain and large vibrating systems, *Proceedings of NOVEM 2005*, Keynote Lecture, St. Raphael, France, 2005.
[3] R.L. Weaver, The effect of an undamped finite degree of freedom 'fuzzy' substructure: numerical solution and theoretical discussion, *Journal of the Acoustical Society of America* 101 (1996) 3159–3164.
[4] R.L. Weaver, Equipartition and mean square response in large undamped structures, *Journal of the Acoustical Society of America* 110 (2001) 894–903.
[5] A. Carcaterra, An entropy formulation for the analysis of power flow between mechanical resonators, *Mechanical Systems and Signal Processing* 16 (2002) 905–920.
[6] A. Carcaterra, A. Akay, Transient energy exchange between a primary structure and a set of oscillators: return time and apparent damping, *Journal of the Acoustical Society of America* 115 (2004) 683–696.
[7] I. Murat Koç, A. Carcaterra, Z. Xu, A. Akay, Energy sinks: vibration absorption by an optimal set of undamped oscillators, *Journal of the Acoustical Society of America* 118 (2005) 3031–3042.
[8] A. Carcaterra, A. Akay, I.M. Koc, Near-irreversibility in a conservative linear structure with singularity points in its modal density, *Journal of the Acoustical Society of America* 118 (2006) 2141–2149.
[9] R.C. Tolman, *The Principles of Statistical Mechanics*, Oxford University Press, New York, 1938.
[10] R.H. Lyon, R.G. De Jong, *Theory and Applications of Statistical Energy Analysis*, second ed., Butterworth-Heinemann, Newton, MA, 1995.
[11] A.I. Khinchin, *Mathematical Foundations of Statistical Mechanics*, Dover, New York, 1949.
[12] E. Fermi, J. Pasta, S.M. Ulam, Studies of nonlinear problems, Los Alamos 1940, 1955, in: E. Fermi (Ed.), Collected Papers II, Vol. 978, Academia de Lincei and University of Chicago Press, 1965.
[13] P.K. Datta, K. Kundu, Energy transport in one-dimensional harmonic chains, *Physical Review B* 51 (1995) 6287–6295.
[14] R. Livi, M. Pettini, S. Ruffo, M. Sparpaglione, A. Vulpiani, Equipartition threshold in nonlinear large Hamiltonian systems: the Fermi–Pasta–Ulam model, *Physical Review A* 31 (1985) 1039–1045.
[15] K. Ullmann, A.J. Lichtenberg, G. Corso, Energy equipartition starting from high frequency modes in the Fermi–Pasta–Ulam β oscillator chain, *Physical Review E* 61 (2000) 2471–2477.
[16] C.H. Hodges, J. Woodhouse, Vibration isolation from irregularity in a nearly periodic structure: theory and measurements, *Journal of the Acoustical Society of America* 74 (1983) 894–905.
[17] R.L. Weaver, O.I. Lobkis, Anderson localization in coupled reverberation rooms, *Journal of Sound and Vibration* 231 (2000) 1111–1134.
[18] F.J. Fahy, Statistical energy analysis: a critical overview review, *Philosophical Transactions of the Royal Society of London Series A* 346 (1994) 437–447.
[19] R.S. Langley, A general derivation of the statistical energy analysis equations for coupled dynamic-systems, *Journal of Sound and Vibration* 135 (1989) 499–508.

[20] E.H. Dowell, D. Tang, Multiscale, multiphenomena modeling and simulation at the nanoscale: on constructing reduced-order models for nonlinear dynamical systems with many degrees of freedom, *Journal of Applied Mechanics* 70 (2003) 328–338.
[21] E.H. Dowell, D. Tang, *Dynamics of very High Dimensional Systems*, World Scientific, Singapore, 2003.
[22] T.T. Soong, *Random Differential Equations in Science and Engineering*, Academic Press, New York, 1973.
[23] Y.K. Lin, G.Q. Cai, Stochastic Analysis of Nonlinear Systems, in: S.G. Braun, D.J. Ewins, S.S. Rao (Eds.), *Encyclopedia of Vibration*, Academic Press, New York, 2002.